
COMMENTS AND ADDENDA

The Comments and Addenda section is for short communications which are not of such urgency as to justify publication in Physical Review Letters and are not appropriate for regular Articles. It includes only the following types of communications: (1) comments on papers previously published in The Physical Review or Physical Review Letters; (2) addenda to papers previously published in The Physical Review or Physical Review Letters, in which the additional information can be presented without the need for writing a complete article. Manuscripts intended for this section may be accompanied by a brief abstract for information-retrieval purposes. Accepted manuscripts will follow the same publication schedule as articles in this journal, and galley proofs will be sent to authors.

Self-Consistent Pseudopotential for Si

Joel A. Appelbaum and D. R. Hamann

Bell Laboratories, Murray Hill, New Jersey 07974

(Received 5 February 1973)

The possibility of self-consistency within the pseudopotential method is demonstrated for Si. A smooth real-space model potential for Si^{4+} is shown to lead to a pseudopotential which is self-consistent with its pseudocharge density in the Hartree-Fock-Slater sense, and gives an energy-band spectrum whose optical gaps agree with experiment.

The successes empirically chosen pseudopotentials have had in the calculation of the energy bands and optical properties of a wide class of solids have been amply documented.¹ Less firmly established is the treatment of pseudocharge densities calculated from these potentials as if they were actual charge densities.² The fundamental difficulty in making this identification is the fact that pseudo-wave-functions lack the oscillations in the atom-core regions which are present in the actual valence wave functions. Walter and Cohen have recently shown that the total pseudocharge in the region of the covalent bond in several semiconductors correlates well with the empirically assigned bond charge.² While this calculation supports the physical significance of the pseudocharge (away from the cores), it raises another question. Walter and Cohen use an empirical pseudopotential whose Fourier components are set equal to zero for reciprocal-lattice vectors larger than (3, 1, 1). This cannot be synthesized into a sensible coordinate-space ion potential. Correspondingly, they take many more Fourier components into account in synthesizing their charge densities. This leaves open the possibility that the pseudocharge density only "works" in combination with a potential with which it cannot be self-consistent. In this paper, we have investigated this question and found that a sensible real-space model potential for Si^{4+} can give a self-consistent pseudopotential and pseudocharge, while simultaneously fitting the experimentally determined band struc-

ture. This lends further support to the physical significance of pseudocharge densities.

A smooth three-parameter model potential for Si^{4+} is constructed as follows: The ionic charge is taken as

$$\rho = 4(\alpha/\pi)^{3/2} e^{-\alpha r^2}$$

and the core potential V_c as

$$(v_1 + v_2 r^2) e^{-\alpha r^2},$$

where v_1 , v_2 , and α are adjustable parameters. The ionic potential is shown in Fig. 1.

The total potential in the solid V_T is the sum of three terms. A Hartree potential V_H is calculated exactly from Poisson's equation. An exchange and correlation potential V_{x-c} is calculated using Slater's exchange approximation with a coefficient adjusted to agree with the Wigner interpolation formula at the average valence-electron density of Si.³ The third term is V_c defined above. Both V_H and V_{x-c} are calculated using the pseudocharge density.

Our aim is to determine a total pseudopotential which has the property that the pseudocharge density it implies, when used as outlined above, generates an identical pseudopotential and at the same time produces energy bands consistent with optical data. We have three adjustable parameters v_1 , v_2 , and α to achieve both these objectives. Our stratagem for determining the Si^{4+} model potential consisted of the following: The model potential was related to the total pseudopotential through

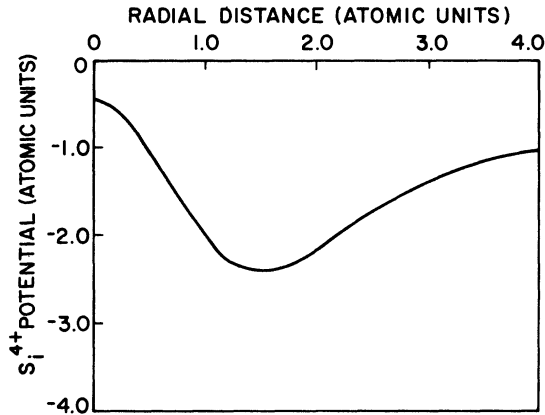


FIG. 1. Si^{4+} -ion potential is plotted vs radial distance for the parameters $v_1=3.042$, $v_2=-1.372$, and $\alpha=0.6102$ which leads to the self-consistent pseudopotential tabulated in Table I.

linear screening including a linearization of the Slater exchange potential as previously discussed by the authors.⁴ The ion-potential parameters were then adjusted to yield a pseudopotential which generated an acceptable energy-band spectrum,⁵ calculated by methods similar to Brust.⁶ That spectrum, shown in Fig. 2, was generated without truncating the pseudopotential $V_T(\vec{G})$ at $|\vec{G}|^2=11$, as is common practice, but by including terms through $|\vec{G}|^2=24$, by which wave vector V_T has decayed almost to zero. The pseudopotential coefficients are listed in Table I. These fall within the family of curves presented by Martin⁷ which give reasonable first-principles phonon dispersion

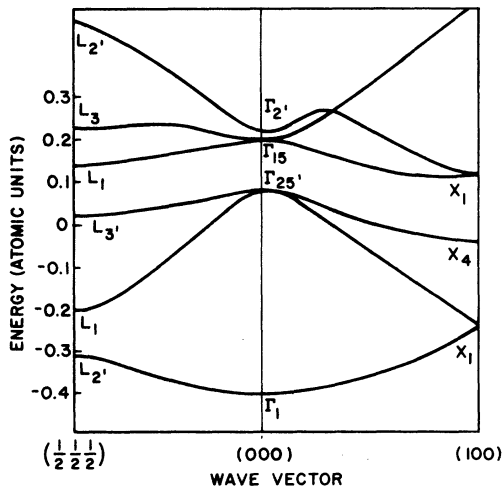


FIG. 2. Energy bands of Si calculated from the potential components of Table I are shown plotted along Γ to X and Γ to L. Main emphasis was placed on valence bands and conduction to valence band gaps.

TABLE I. Values of the pseudopotential form factors $V_T(|\vec{G}|^2)$ for this calculation and those quoted by Cohen and Heine.^a

Pseudopotential	$V_T(3)$	$V_T(8)$	$V_T(11)$	$V_T(16)$	$V_T(19)$	$V_T(24)$
Present calculation	-0.1051	0.0246	0.0401	0.0349	0.0277	0.0171
Cohen and Heine ^a	-0.1055	0.0201	0.0403	0.0	0.0	0.0

^aM. L. Cohen and V. Heine, in Ref. 1, p. 190.

curves for Si. The pseudocharge density was then calculated and used to generate both the Hartree potential V_H and the exchange and correlation potential V_{x-c} . These terms together with V_c form a new total potential V_T which we compare with our starting potential to determine how close to self-consistency we have come.

The input and output potentials are shown in Fig. 3. We have exhibited the bulk Si potentials in what is known as a mixed or Laue representation,

$$V(\vec{x}) = \sum_{\vec{G}_n} V_{\vec{G}_n}(z) e^{i\vec{G}_n \cdot \vec{x}_n},$$

where the coordinate z in this case is along the body diagonal of the crystallographic unit cell for Si and \vec{G}_n is the projection of the reciprocal-lattice vector on the (111) plane. We will label \vec{G}_n by pairs of integers denoting its components in the orthogonal basis $\vec{u}_1 = (1/\sqrt{2})(\hat{a}_1 - \hat{a}_2)$, $\vec{u}_2 = \frac{1}{3}(1/\sqrt{2}) \times (\hat{a}_1 + \hat{a}_2 - 2\hat{a}_3)$, where \hat{a}_n , $n=1, 2, 3$, are the crystallographic unit vectors. This choice of representation was necessitated by the computer codes that were used to calculate $V_T(\vec{x})$ and $\rho(\vec{x})$, which were written to perform a self-consistent calculation of the (111) surface of Si.⁸ It has the added advantage of giving a more pictorial representation of the total real-space potential than would be achieved by just exhibiting the pseudopotential coefficients $V_T(\vec{G})$. The input potential shown in Fig. 3 was calculated by Fourier synthesizing the $V_T(\vec{G})$ used in the calculation of the energy bands. It should be mentioned that the energy bands were also calculated using the transfer-matrix technique directly^{8,9} from the input potential $\{V_{\vec{G}_n}(z)\}$, obtaining essentially the same results as are shown in Fig. 2, and it was from the wave functions generated in this way that $\rho_{\vec{G}_n}(z)$ was calculated. The charge density was calculated from an eight-point sampling including the Γ , X, L symmetry points of the Brillouin zone. This scheme, used initially by Kleinman and Phillips,¹⁰ has been shown to give good convergence.¹¹

Turning to a comparison of the input and output potentials, we see there is remarkably close agreement between the two potentials. The maximum discrepancy is ~ 0.01 a.u. in the $V_{11}(z)$ potential, which, if one Fourier analyzes this potential along

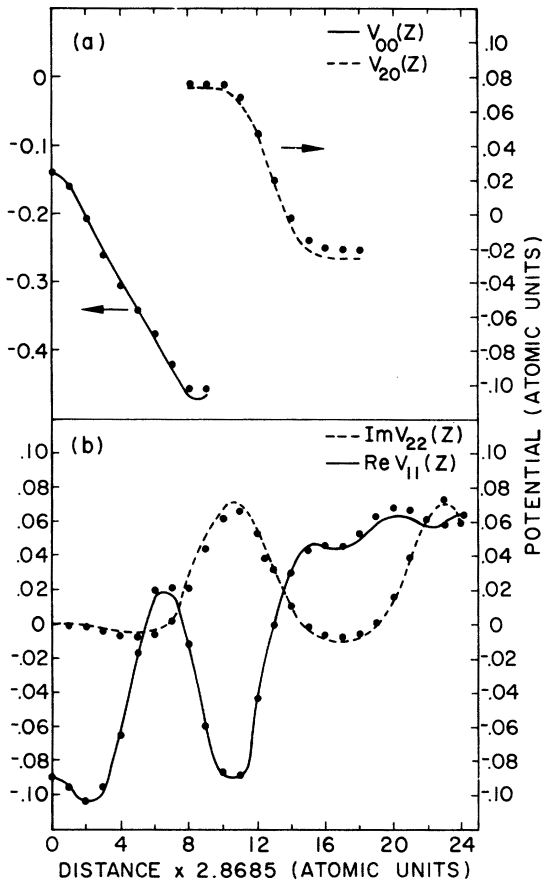


FIG. 3. Input potentials (solid or dashed lines) and output potentials (solid dots) are compared for (a) the $V_{00}(z)$ and $V_{20}(z)$ potentials and (b) the $\text{Im}V_{22}(z)$ and $\text{Re}V_{11}(z)$. The distance z is measured along the body diagonal, where 0 to 17 represents one-third the crystallographic body diagonal. In part (a), only portions of $V_{00}(z)$ and $V_{20}(z)$ have been plotted since the potential has mirror symmetry. Note the fact that the energy scales of (a) for $V_{00}(z)$ and $V_{20}(z)$ are different.

the z direction, would lead to a discrepancy for $V_T(1, 1, 1)$ between its input and output value of 0.0035 a.u. or < 0.1 eV.

The consistency we have achieved between input and output potentials has two important implications. The first is that one need not be content with adjusting the first few pseudopotential parameters (assuming the rest zero) in what *a priori* might appear a rather arbitrary fashion in order to empirically fit the important energy gaps in a particular material. Rather, adjusting the few physical parameters characterizing the Si^{4+} -ion

potential allows one to achieve both a good fit to the energy gaps and self-consistency. While our emphasis on the efficacy of a model potential in this context is hardly new,¹² we believe the demonstration of self-consistency is strong argument in its favor.

The second point we wish to make concerns the role of linear-response theory in our starting the self-consistency loop. Clearly it is remarkably successful in achieving an excellent starting potential. The same cannot be said for the charge density. The charge density calculated by linear-response theory is deficient in two important respects. First, the allowed Fourier components of the charge density differ from their linear-response values: $\rho(3)$ by $\sim 10\%$ and the higher component such as $\rho(11)$ by a factor of 2. Second, the "forbidden" Fourier components of charge density, such as ρ_{222} , are not unimportant. These forbidden components are a clear manifestation of the nonlinear relationship between charge and potential, since there is essentially no V_{222} potential. It is common¹³ to ascribe the presence of ρ_{222} charge density to a bond-charge model where one puts δ -function charge distributions at the center of the bonds between Si atoms. The main function ρ_{222} fulfills, insofar as we can tell, is to ensure that the regions where the charge density is small remain positive definite. This is not in the region where the bond charge is present [coming from $\rho(3)$], on the contrary it is as far away as one can get from the bond charge. Furthermore, it is just these regions where linear-response theory leads to a negative charge density.

At this point the reader may be wondering why there is no $V_T(222)$ forbidden potential when one has significant ρ_{222} charge components. This is accounted for by the fact that the Hartree potential produced by a comparatively rapidly varying charge disturbance is quite small, coupled with a cancellation of approximately half the Hartree potential by the exchange and correlation potential.

In conclusion, while there have been a number of *a priori* self-consistent calculations for Si,^{10,14} this is the first to have demonstrated that it is possible to construct a smooth and physically reasonable real-space model potential for Si^{4+} which leads to self-consistent energy bands and charge densities in the context of a pseudopotential calculation.

We would like to acknowledge a number of useful discussions with E. O. Kane, J. C. Phillips, and J. A. Van Vechten.

¹M. L. Cohen and V. Heine, in *Solid State Physics*, edited by F. Seitz, D. Turnbull, and H. Ehrenreich (Academic, New York, 1970), Vol. 24, pp. 38-249.

²J. P. Walter and M. L. Cohen, *Phys. Rev. Lett.* **26**, 17 (1971).

³This leads to a value of 0.76 for the constant relating V_{x-c} and $\rho^{(1/3)}$ in units where Slater's choice is 1.

⁴J. A. Appelbaum and D. R. Hamann, Phys. Rev. B **6**, 2166 (1972).

⁵M. L. Cohen and T. K. Bergstresser, Phys. Rev. **141**, 789 (1966).

⁶D. Brust, Phys. Rev. **134**, A1337 (1964).

⁷R. Martin, Phys. Rev. **186**, 871 (1969).

⁸J. A. Appelbaum and D. R. Hamann (unpublished).

⁹P. M. Marcus and D. N. Jepsen, Phys. Rev. **20**, 925 (1968).

¹⁰L. Kleinman and J. C. Phillips, Phys. Rev. **118**, 1153 (1960).

¹¹W. Brinkman and B. Goodman, Phys. Rev. **149**, 597 (1966).

¹²See Sec. 10 of Ref. 1 for a review of the relevant literature on model potentials.

¹³J. C. Phillips, *Covalent Bonding in Crystals, Molecules, and Polymers* (University of Chicago Press, Chicago, 1969).

¹⁴D. J. Stukel and R. N. Euwema, Phys. Rev. B **1**, 1635 (1970).

Magnetic Susceptibility of the Noble Metals around Their Melting Points

R. Dupree and C. J. Ford

Physics Department, University of Warwick, Coventry, England

(Received 2 October 1972)

The magnetic susceptibilities of the noble metals have been accurately measured close to the melting point in both liquid and solid states. In the liquid the susceptibilities are (in cgs volume units) Cu: $(-0.70 \pm 0.01) \times 10^{-6}$, Ag: $(-2.05 \pm 0.01) \times 10^{-6}$, Au: $(-2.74 \pm 0.01) \times 10^{-6}$, and in the solid Cu: $(-0.59 \pm 0.01) \times 10^{-6}$, Ag: $(-1.84 \pm 0.01) \times 10^{-6}$, Au: $(-2.63 \pm 0.01) \times 10^{-6}$. The results obtained agree well with the susceptibilities calculated recently by Borchì and de Gennaro if the effects of electron-electron interactions are correctly taken into account.

There is considerable uncertainty in the experimental values for the magnetic susceptibility of the liquid noble metals.¹ For instance, different authors obtain opposite sign changes in the susceptibility for copper on melting. Knowledge of the spin susceptibility is important in the interpretation of the Knight shifts in these metals.^{2,3} Furthermore, Borchì and de Gennaro⁴ have recently calculated the electronic susceptibility of the noble metals in both liquid and solid state using a pseudopotential method. They predict that, even in the liquid, there are considerable deviations from free-electron behavior with the paramagnetic term being enhanced and the diamagnetic term reduced. We have therefore made measurements by the Faraday method of the magnetic susceptibility of high-purity (99.999% or better) copper, silver, and gold through their melting points. The values obtained were highly reproducible and the samples showed no sign of oxidation or contamination.⁵ The results are given in row 5 of Table I for the liquid metals and in row 9 for the solid metals. The values for the liquid-metal susceptibility are all more paramagnetic and the changes on melting smaller than the mean of the earlier measurements.¹ The value for copper agrees with a recent measurement of Collings⁶ and that for silver is within the spread of earlier measurements. The only previous measurement for gold⁷ was made rather long ago. Our values are compared with those deduced theoretically in Table I. The effect of the ions on the noninteracting electronic susceptibility has been taken from Borchì and de Gennaro,⁴ who took into account the effects of

electron-electron (ee) interactions on the spin susceptibility χ_p , using the calculation of Silverstein.⁸ However, recent calculations^{9,10} have shown that Silverstein seriously underestimated this effect on χ_p and we have therefore used the results of these calculations to obtain a theoretical estimate of χ_p [i. e., $\chi_p = \chi_p^{free} (1 + \Delta_p)$ ($\chi_{p,ee}/\chi_p^{free}$), where Δ_p takes into account the effect of the ions and $\chi_{p,ee}/\chi_p^{free}$ is the ratio of the susceptibility including ee interactions to the noninteracting susceptibility.] The effects of ee interactions on the diamagnetic susceptibility have been included using the calculation of Kanazawa and Matsudawa,¹¹ although the change in the total electronic susceptibility due to this is small (less than 4% in all cases). The theoretical electronic susceptibility χ_e is given in row 3 for the liquid metals and row 7 for the solid metals, and the free noninteracting value χ_{e0} is given for comparison in row 2. It can be seen that the effect of interactions is considerable. The ion-core values χ_i (row 1 and 6 of the table) are those used in Ref. 1, where it was shown that values calculated using modern free-atom wave functions did not give consistent χ_e values for most metals. The total theoretical susceptibilities are given for the liquid in row 4 and in row 8 for the solid metals. For silver the agreement between theory and experiment is very good in both liquid and solid states and the agreement is also very good for solid copper, although the theoretical change in melting is a bit too large. For gold the apparent agreement is poor; however, the ion-core susceptibility of gold is the largest of any metal and any error in this will dominate the susceptibility. If